Journal of the Geological Society, London, Vol. **150,** 1993, pp. 885–896, 9 figs. Printed in Northern Ireland

Incremental caldera collapse of Suswa volcano, Gregory Rift Valley, Kenya

I.P. SKILLING
Environmental Science Division, Lancaster University, Bailrigg, Lancaster LA1 4YQ, UK
Present address: British Antarctic Survey, Natural Environment Research Council, High Cross, Madingley Road, Cambridge CB3 OET, UK

Abstract: Suswa volcano, located at 1°10′S, 36°20′E, is Quaternary in age (<0.4 Ma), dominantly trachytic–phonolitic in composition, and has two calderas. Regional extension was a fundamental control on caldera collapse, providing pathways for the siting, drainage and recharge of magma chambers. Caldera I collapse was associated with magmatic overpressure from volatile exsolution, magma–water interaction, influx of denser magma and magma drainage at depth. Trachybasalt ash, trachyte globular-ash ignimbrites, trachyte pumice lapilli air-fall tuffs and carbonate-trachyte ignimbrites characterize the initial subsidence. Air-fall tuffs, erupted during caldera collapse at Longonot, are interbedded, suggesting a regional collapse event. Incremental, but dominantly Valles-type, collapse continued with the eruption of trachyte agglutinate flows from concentric ring-fractures outside the caldera ring-fault (Ring-Feeder Zone) and trachyte pumice lapilli air-fall tuffs from west caldera I.

Following caldera I collapse, phonolite lava flows were erupted from the caldera floor. Centrally-erupted phonolite lava flows led to the construction of Ol Doinyo Onyoke lava cone. A pit-crater on the cone was a precursor to the collapse of caldera II, both of which were generated entirely by magma withdrawal. Regional decompression caused ring-fault bounded, block-resurgence of the caldera floor

Suswa volcano, located within the inner graben of the Gregory Rift Valley, Kenya (Fig. 1) at 1°10′S, 36°20′E, is Quaternary in age (<0.4 Ma), dominantly trachytic–phonolitic in composition, and has two calderas. It has a shield morphology with flanks sloping typically <5°, a summit altitude of 2356 m, and its deposits cover an area of >1200 km^2. McCall & Bristow (1965) produced a reconnaissance stratigraphy and geological map, and a more detailed account was given by Johnson (1969), who distinguished seven phases in the growth of the volcano (Table 1), with summaries by Williams *et al.* (1984) and Macdonald (1987). The globule ignimbrites have been studied by Johnson (1968), Schmincke (1972, 1974), Hay & Hildreth (1976) and Hay *et al.* (1979).

Several similar trachyte–phonolite caldera volcanoes occur in Antarctica, e.g. Mount Erebus (Moore & Kyle 1990), Mount Sidley (Le Masurier 1990) and Mount Hampton (Le Masurier & Kawachi 1990), but descriptions are not common. In this paper the evolution of Suswa is re-interpreted and the mechanisms of caldera development are considered.

History

The evolution of Suswa volcano has been divided into eight stages (S1–S8) which are reflected in successive stratigraphic formations (Table 1). The evolution is dominated by two caldera-forming events.

Pre-caldera I volcanism (S1)

The S1 or Angat Kitet Formation comprises mainly undersaturated trachyte lava flows emplaced prior to the development of caldera I. Baker *et al.* (1988) suggested that the Barajai Trachytes, exposed close to the SE flank of Suswa, probably represent the earliest Suswa lavas, but these have not been re-examined. The S1 formation is best exposed in the northeast wall of caldera I at BJ094780 (Fig. 2), where 30 m of highly vesicular, trachyte lava flows and a <2 m thick pumice lapilli tuff crops out. The lavas dip at <10°, from the centre of caldera I. On the southeast flank, the formation is represented by lava domes and a scoria cone (Soitamrut). At least 6 lava domes are aligned in a NNW–SSE direction over a distance of about 2 km to the southwest of Soitamrut.

The tuffs in the northeast wall of caldera I and at Soitamrut are the only record of pyroclastic activity at this time. As Johnson (1969) suggested, it is possible that some of the unconsolidated, fluvial, pumiceous sediments of the lower north flank and the Angat Kitet plains are partly reworked pre-caldera I pyroclastic deposits. Extensive dissection of S1 volcanics, as shown by gulleyed surfaces and an overlying palaeosol (Fig. 3), indicates that a prolonged period of quiescence followed their eruption. Johnson (1969) suggested that the early form of Suswa was a low-angled shield, but there is insufficient evidence to corroborate such a centre.

Recognition of syn-caldera I volcanics

Johnson (1969) indicated the problems of recognizing syn-caldera I deposits. The S3 and S4 formations mantle and are truncated by different sections of the northern walls of caldera I, which implies either that they were erupted during incremental subsidence of the cauldron block(s), or that parts of the caldera walls slumped prior to the S6 (post-caldera I) eruptions. He noted that deposits apparently truncated by the caldera may be banked against

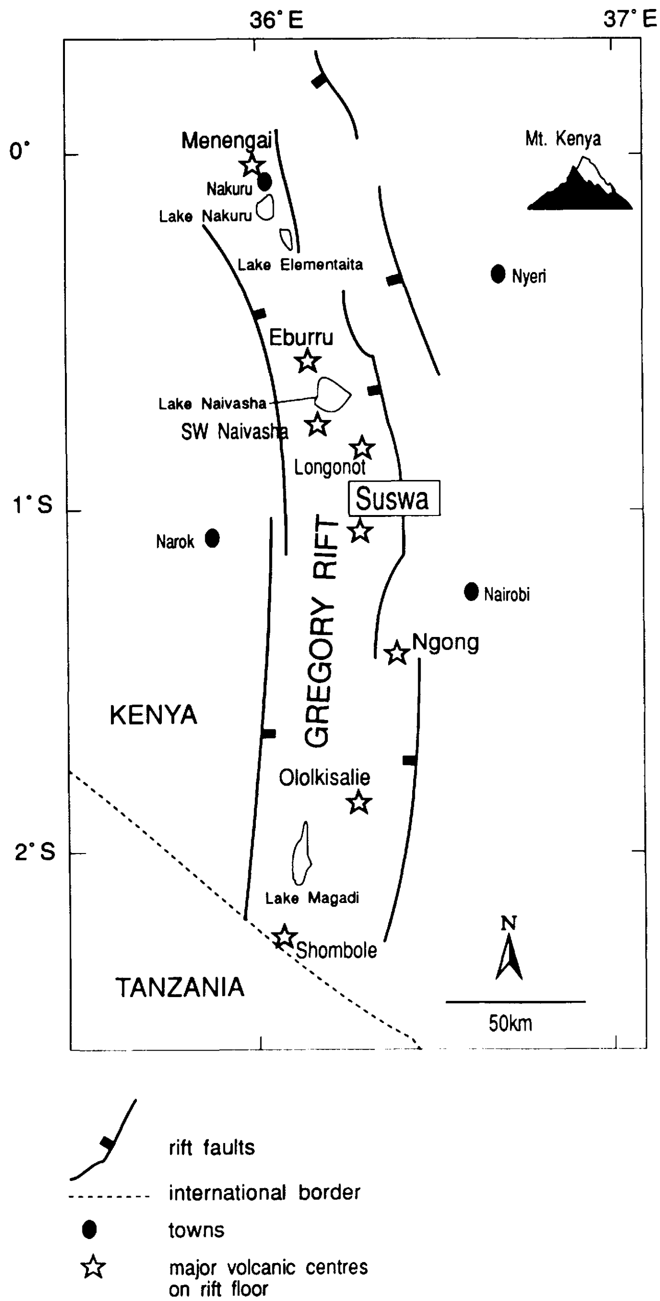

Fig. 1. Location of Suswa volcano in the Gregory Rift Valley, Kenya.

the caldera walls at depth (i.e. post-caldera), but obscured by later post-caldera fill. Whilst it is possible that the S3 and S4 formations are post-caldera I in age, there are several lines of evidence to suggest that this is not the case. All unequivocal pre-caldera I deposits at Suswa are trachytic and unequivocal post-caldera I deposits are phonolitic. The S2–S5 formations are all trachytic and clearly overlie the pre-caldera S1 unit. The S2 formation comprises pyroclastic deposits with the widest compositional range (trachybasalt–trachyte), suggesting a significant change of the feeder system and eruption dynamics in the initial stages of caldera collapse. The S3 formation was erupted from ring-fractures (Ring-Feeder Zone, RFZ), concentric with the caldera-ring-fault, suggesting contemporaneous development. At least part of the S4 formation was also erupted from this fracture zone. The S5 formation overlies S4 pumice-lapilli tuffs and has been assigned to syn-caldera I because of its trachytic composition.

Syn-caldera I volcanism (S2–S5)

Syn-caldera I deposits are divided into four formations (S2-S5).

Olgumi Formation (S2). This formation, <20 m thick, displays the widest compositional range (Fig. 3). It consists of trachyte pumice-lapilli tuffs, trachybasaltic ash and spatter deposits, mixed carbonate-trachyte tuffs and two deposits termed 'globule ignimbrites' by Hay *et al.* (1979).

The *globule ignimbrites* are 0.5–2.5 m thick, with >80% of trachytic, globular ash, and are best exposed on the northeast and southeast flanks. Both deposits have aspect ratios of approximately 1:20 000 (the aspect ratio is a ratio of average vertical thickness to horizontal extent (H), where H is the diameter of a circle with the same surface area as the deposit). The ignimbrites thin upslope and thicken into depressions, with some rheomorphic folding on valley sides. They are welded at their bases and cemented by vapour-phase anorthoclase at higher levels. The ignimbrites are typically columnar-jointed and contain 'volatile-blisters', up to 15 m across, which are similar to those described on Fantale, Ethiopia (Gibson 1970, 1974) and in the Bishop Tuff, California (Sheridan 1976).

Both ignimbrites on the upper flank have a basal zone, 4–15 cm thick, with grey–black, vitric lenses, up to 4 cm long in a homogeneous grey–brown matrix of 80–85% of trachytic, vitric ash globules, with <1% of anorthoclase crystals and microsyenite clasts. An upper dark-brown zone is locally overlain by a <5 cm thick palaeosol. Subspherical vesicles, up to 4 cm in diameter, are present throughout, and increase in size toward the top of each ignimbrite. They have a drusy appearance due to vapour-phase crystallization (dominantly anorthoclase) on the walls. The globules are often colour-zoned, banded and have 'budded' margins (Hay *et al.* 1979).

Three mixed *carbonate–trachyte tuffs*, exposed on the north and southeast flanks are included in the Olgumi Formation (Fig. 3). They are <2.5 m thick, pale yellow to yellow–brown, unwelded, but weakly consolidated due to primary and secondary carbonate cementation. All three tuffs thicken into depressions and the lowest tuff has stoss-side concentrations of coarser clasts behind volatile blisters in the underlying globule ignimbrites. Locally infilled, polygonal desiccation cracks occur on the upper surfaces. The basal contacts are sharp only where the tuffs overlie S1 lavas or globule ignimbrites. Where they overlie trachybasaltic ashes, rounded blebs of carbonate–trachyte ash are detached from their bases and are intermixed with the trachybasaltic ash.

The ashes contain globules of carbonate and trachyte ash (<100%), trachytic pumice lapilli (<10%), anorthoclase (<2%) and syenite and trachyte lithics (<2%). Rare, basal concentration zones of coarse pumice (>3 cm; <50%) and anorthoclase megacrysts (>0.5 cm; <50%) have been distinguished (Fig. 4). On the northeast flank, localized areas with pristine trachyte and carbonate globules,

Table 1. *Summary of geological evolution of Suswa*

Relationship to caldera collapse	New formations	Johnson (1969) subdivisions	K-Ar dates[a] Ma BP	Volumes (dre)[b] km^3	Summary of geological history
Post-caldera II resurgence	S8 Eululu	Ring Trench floor lavas and south flank lava		>0.1	Recent eruptions of phonolite lavas from SE Ring Trench and south flank
Post-caldera I Syn-caldera II Post-caldera II	S7 Ol Doinyo onyoke	Ol Doinyo Nyukie lavas		>16	Construction of Ol Doinyo Onyoke cone (S7); magma withdrawal generating pit-crater then collapse of caldera II. Caldera floor breccias (S7) from collapse of this cone; eruption of caldera floor phonolite lava flows (S7); block resurgence
Post-caldera	S6 Entarakua	Early postcaldera lavas	0.1 ±0.01	>11	Eruption of phonolite lave flows from vents on floor of caldera I; overtopping of eastern and southern margins of caldera I
Syn-caldera I (?)	S5 Enkorika			<0.05	Development of N flank N–S fissure zone (Enkorika Fissure Zone) with eruption of low-volume trachytic lava flows and domes
Syn-caldera I	S4 Esinoni	Bedded pumics deposits		>7.1	S3 trachytic aggultinate flow eruptions from RFZ; S4 airfall pumice lapilli tuffs from west caldera I vent(s); subsidence of cauldron block(s) in NW; continued incremental subsidence
Syn-caldera I	S3 Oloolwa	Ring-feeder laves		>1.5	
Syn-caldera I	S2 Olgumi	Lahars Globule-surface lavas[c] Globule flows[c]		>1.8	Influx of water into RFZ; magma-water interaction; lateral propagation of trachybasaltic magma; RFZ eruptions and initiation of incremental caldera collapse; interbedding of Longonot syn-caldera pumice
					Quiescence
Pre-caldera I	S1 Angat kitet	Primitive shield lavas	0.24 ± 0.01	>4	Fissure eruptions on graben floor (?) led to development of a shield or complex of vents; development of RFZ (and an earlier caldera?)

[a] Baker *et al.* 1988.
[b] Dense rock equivalent.
[c] See text for explanation of terms.
RFZ Ring Feeder Zone

intermixed in highly variable proportions, are preserved. But at most localities, carbonate is present only as matrix cement. The petrography and geochemistry of the ashes are described in detail in Macdonald *et al.* (1993)

Trachybasaltic vitric ash and spatter deposits are interbedded between two carbonate-trachyte tuffs on the northeast flank (Fig. 3). They are up to 2.5 m thick, poorly consolidated, well-sorted, dark green to black and locally parallel-laminated. Grey clay beds, <2 cm thick, with desiccation cracks, are locally present within the ashes on the upper northeast flank. The ashes consist of angular, unvesiculated, vitric clasts (<90%), accretionary and armoured lapilli (<40%), and pumice lapilli (<10%).

Trachyte pumice-lapilli tuffs are also present in the Olgumi Formation (Fig. 3). They are thin (<3m thick), clast-supported, with crude normal grading, though basal reverse grading is present at some localities.

Interpretation of S2 Formation. The *globule ignimbrites* were termed 'globule flows', 'bubble flows' and 'globule-surface lavas' by Johnson (1966, 1968, 1969). He suggested

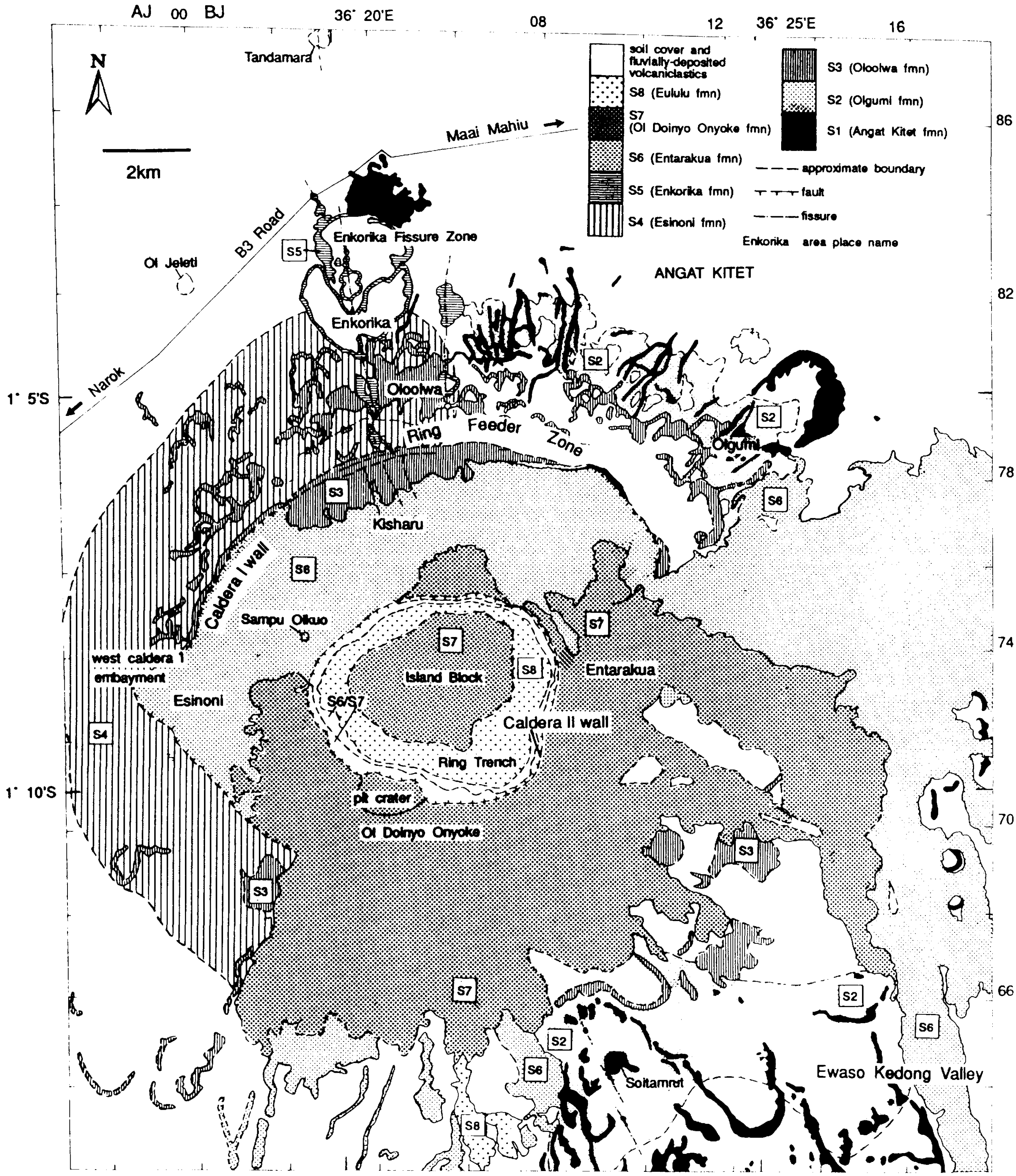

Fig. 2. Geological sketch map of Suswa (with Survey of Kenya grid).

they were generated by vesiculation of the upper layer of a lava flow ('globule-surface lava') and flowage of this surface layer downslope ('bubble flow' or 'globule flow'). However, Schmincke (1972, 1974), suggested an ignimbritic origin. Hay *et al.* (1979) noted the presence of a thin palaeosol separating the flows from the underlying lavas, and also interpreted them as ignimbrites, introducing the term 'globule ignimbrite'.

Globular pyroclasts can be produced by several mechanisms: liquid immiscibility (Hamilton *et al.* 1979), fire-fountaining (Keller 1981), melting of shards in an eruptive cloud (Schmincke 1974; Heiken & Lofgren 1971),

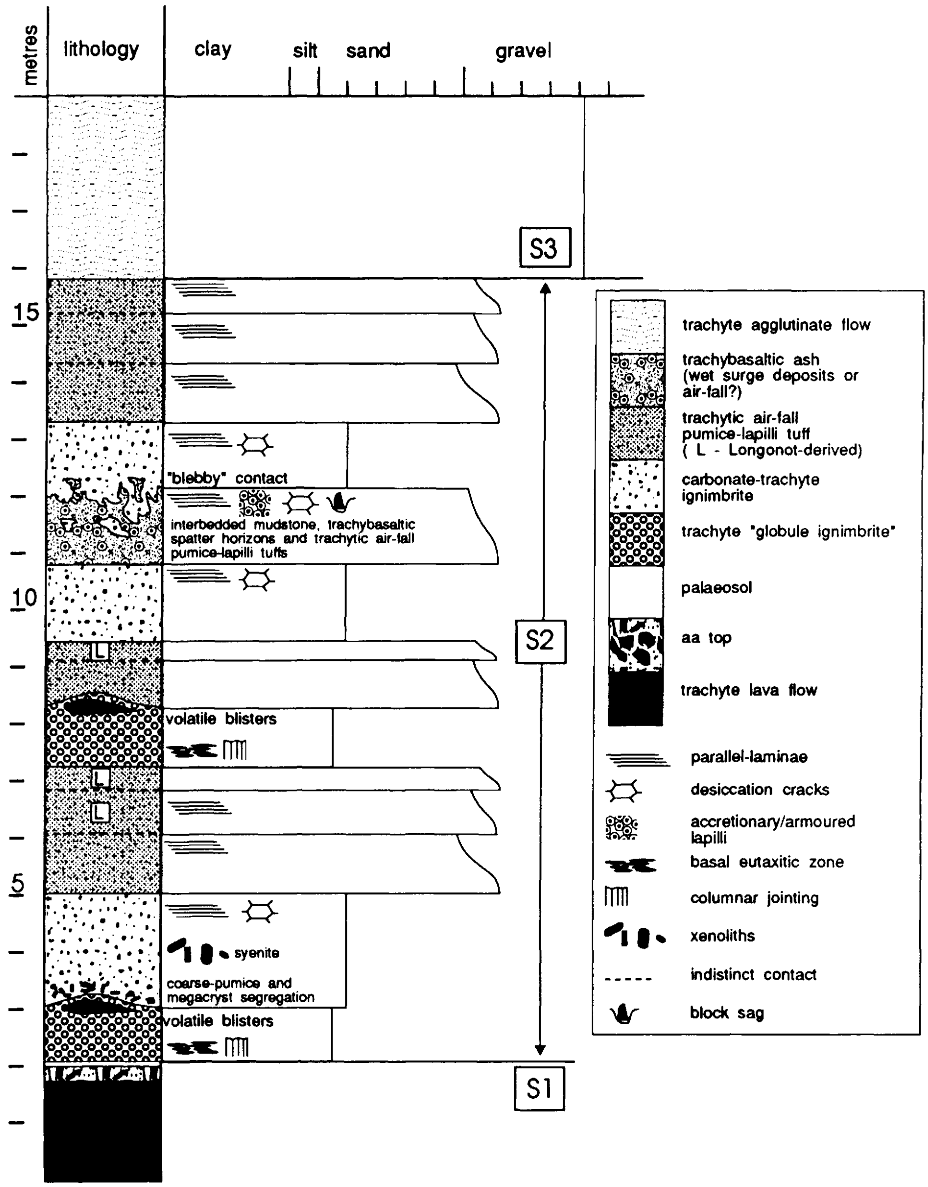

Fig. 3. Composite log of Olgumi (S2) formation.

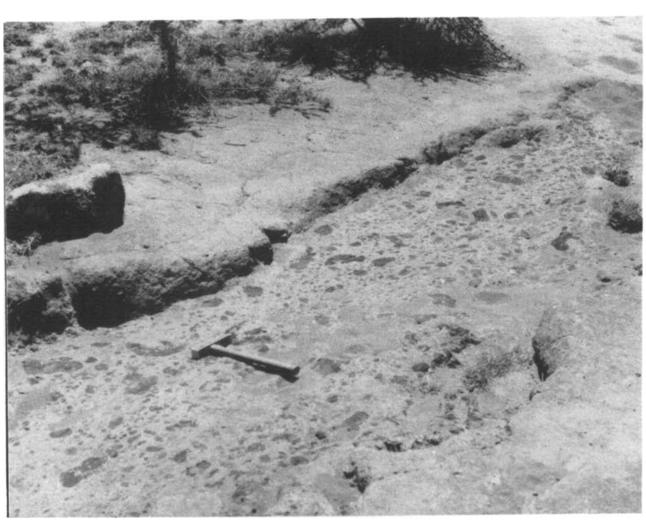

Fig. 4. Coarse pumice segregation in S2 carbonate–trachyte ignimbrite at BJ119769 (hammer is 35 cm long).

and phreatomagmatic explosion (Wohletz 1983; Zimanowski *et al.* 1986). They occur most frequently in air-fall ashes of low viscosity and basaltic composition, but rarely occur as discrete clasts, usually adhering to the surface of larger, non-globular, particles.

The argument for an origin by liquid immiscibility rests on the similarity of the globules to those in the associated carbonate–trachyte tuffs, in which there is petrographic and geochemical evidence for liquid immiscibility (Macdonald *et al.* 1993). No carbonate is present in the globule flows, and post-eruptive dissolution is necessary to explain its absence. As the glass is very fresh, this mechanism is unlikely. Formation by fire-fountaining is also unlikely as the colour zoning, banding, and convoluted margins of the globules, contrast strongly with the smooth-surfaced homogenous spheres associated with such activity (Keller 1981).

An origin by melting of angular shards in a hot eruptive cloud was suggested by Schmincke (1974). A similar origin is also implied by comparison with globules in lunar regolith. Both smooth-surfaced/homogeneous and convolute-surfaced/budded, colour-zoned globules occur in lunar regolith. Heiken & Lofgren (1971) suggested that convolute-surfaced lunar globules were produced by quick melting of small particles within a fireball, and the more homogeneous type by activity analogous to fire-fountaining. Angular shards are extremely rare in the Suswa deposits, arguing against these hypotheses.

Support for a phreatomagmatic origin comes from the high content of ash, the association with trachybasaltic ashes (which contain numerous accretionary lapilli) and the occurrence of volatile blisters which may have been generated by trapped surface water. A wide range of pyroclast shapes and surface textures is known to occur in phreatomagmatic deposits. Wohletz (1983) found that the percentage of globular particles increased with decreasing grain-size and increasing amounts of water in thermite–water explosions. If a similar process operated during the formation of the youngest globule-bearing deposit, for example, a minimum water volume, either ground or surface water, of about 0.1 km^3 would be required.

The timing of volatile exsolution relative to eruption and emplacement may also be critical. The highly expanded vesicles, which increase in size toward the top of the flows, suggest that abundant volatile exsolution took place after emplacement in the Suswa flows. Wohletz (1983) argued that the bursting of vesicle bubbles would fragment magma and propel it into a magma–water mixing zone, where rapid vapourization of water and brittle fracturing of shards would occur. Limited volatile exsolution of the globule ignimbrites prior to emplacement probably prevented brittle fracturing of pyroclasts. A rapid eruption and emplacement rate would be necessary to ensure post-emplacement exsolution of volatiles on such a scale.

In conclusion, the field evidence is consistent with generation of the globule ignimbrites by phreatomagmatic interaction of a low-viscosity, volatile-rich, trachyte melt, with an aquifer or surface body of water. The eruptions were of high explosivity (suggested by their grain size and aspect ratios) and eruption rate, and were emplaced as pyroclastic flows.

The *carbonate–trachyte* tuffs display valley-thickening and stoss-side concentrations of coarse pumice (Fig. 4) and anorthoclase crystals, suggesting that they were emplaced as flows. Johnson (1966, 1969) interpreted them as lahars, or water-fluidized (<100 °C) debris flow deposits, in the sense of Walker (1983). Desiccation cracks present on the top surface indicate shrinkage of water-saturated material. The 'blebby' contacts with the trachybasaltic ashes could have been generated by loading of water-saturated deposits. Carbonate, anorthoclase megacrysts and syenite lithics are all juvenile, suggesting that if they are lahars, they must be primary deposits. However, an ash-flow (i.e. gas-fluidized) origin is proposed, because no coarse-pumice and crystal concentration zones of the type seen at Suswa have been described from lahar deposits. The extreme localization of these zones suggests an origin by elutriation of fines due to gas streaming, or in vortices associated with topographic irregularities. They do not represent a fines-depleted ground layer (Wilson 1980; Wilson & Walker 1982) because of their localized nature. If an ash-flow origin is accepted, the 'blebby' contacts could be due to high-temperature fluidization of the underlying ash. Water-saturation, indicated by desiccation cracks, may have been due to rainwater or condensed steam. The lack of welding suggests that although the flows were gas-fluidized, they were emplaced at a relatively low temperature (100–500 °C?) or that their heat was lost rapidly after deposition.

The pristine nature of the trachyte in association with carbonate and the globular nature of both phases suggest liquid immiscibility. This is supported by similar chondrite-normalized REE patterns and $^{143}Nd/^{144}Nd$ values of the carbonate and trachyte and high F abundances in the carbonate (Macdonald *et al*. 1993).

The *trachybasaltic ashes and spatter beds* were probably generated by alternating phreatomagmatic and strombolian activity. The presence of surface water is suggested by the interbedded laminated grey clay horizons, interpreted as suspension deposits. As there is no evidence that the associated globule ignimbrites or carbonate–trachyte ashes were emplaced subaqueously; surface water was probably ephemeral or generated as a consequence of the eruptions.

The trachybasaltic ashes could have been emplaced either as air-fall from clouds of water-rich ash, or from poorly expanded wet surges. Vesicles, representing trapped steam in a cohesive matrix, commonly occur in wet surge deposits (Lorenz 1974) but are much rarer in air-fall deposits. The evidence is ambiguous but the very good sorting and the absence of vesicles in the Suswa ashes suggest an air-fall origin. Some of the ashes with very well developed planar laminae may have been deposited subaqueously in ephemeral lakes. The presence of accretionary lapilli does not exclude subaqueous emplacement (Bateson 1965; Lowe & Knauth 1978).

The *trachyte pumice-lapilli tuffs* in the S2 formation are likely air-fall deposits.

Oloolwa Formation (*S*3). The S3 formation is dominated by trachyte flows with an average aspect ratio of 1:300, which extend only up to 4 km from the caldera scarp. Most of the flows have shallow dips (5–10°) with contorted flow folding on the steeper slopes of the caldera margin (Fig. 5).

The flows display complex, convoluted, centimetre-scale banding, reflecting variations in grain size, vesiculation and abundance of vapour-phase anorthoclase. In the upper part, highly irregularly-shaped cavities, <1–15 cm across, lined with vapour-phase anorthoclase are locally well developed. The cavities are similar to those developed in the upper zones of the S2 globule ignimbrites, but are much

Fig. 5. Contact of flow-folded S3 trachyte agglutinate flow with underlying S3 trachyte pumice-lapilli air-fall tuffs at BJ076780 (hammer is 35 cm long).

more irregular in shape. Subrounded, devitrifed pumice clasts (<1–10 cm across) form up to 15% of the rock.

Interpretation of S3 Formation. The textures in S3 flows closely resemble those in some S4 trachyte flows which grade both laterally and vertically into welded air-fall units. The complex textural heterogeneity and the high percentage of vesicular pumice clasts, suggest an agglutinate flow origin. The highly viscous nature of some flows is suggested by the contorted flow folding.

Esinoni Formation (S4). The Esinoni Formation is restricted to the western flanks of Suswa and the walls of the western caldera I embayment. It is dominated by <2.5 m thick, trachyte pumice lapilli tuffs, but over a wide area the base is marked by parallel-laminated grey ash, and the top by a thin sequence of laminated ashes with erosion channels, rip-up clasts, pumice lapilli lenses and cross-laminations (Fig. 6). Most tuffs are well-sorted, normally graded and separated by palaeosols.

Thin trachyte flows are also present throughout the unit. They grade vertically and laterally, to coarse welded air-fall units (Fig. 6). At several localities on the west flank, flows grade laterally into isolated lenses of similar material.

Parallel-laminated ashes with interbedded lenses of pumice-lapilli tuff are the youngest S4 deposits, best exposed on the northwest rim of caldera I (Fig. 7). The tuffs display low-angled (<10-20°), cross-laminated, dune-like bedforms, soft sediment deformation and rip-up blocks. The axial traces of dune structures are perpendicular to the caldera margin. They also contain channels, <50 cm–1 m in diameter, up to 1m in depth, with steep sides (60-80°), rounded bottoms and long axes approximately parallel to the caldera I margin. Some of the channels are asymmetrical but most have a U-shaped profile.

Fig. 7. S4 trachyte dry surge deposits, illustrating surge-eroded (?) channels at AJ989732 (50 cm bar scale).

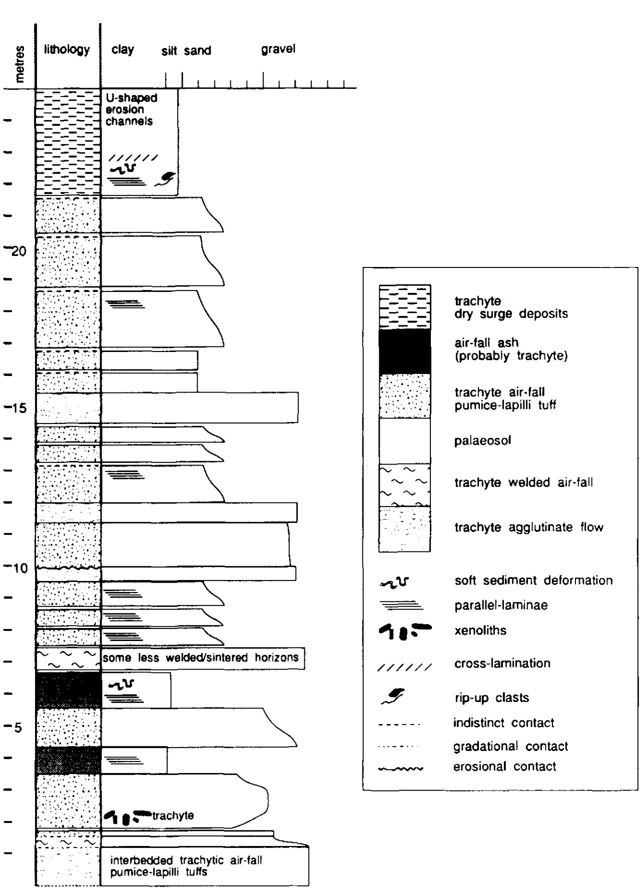

Fig. 6. Log of Esinoni (S4) formation at AJ997750.

Interpretation of S4 Formation. The dominant pumice-lapilli tuffs are clearly of air-fall origin. The thin beds and the numerous interbedded palaeosols suggest a series of sporadic low-volume eruptions. The absence of any significant dissection suggests that periods of inactivity were of short duration, and that the palaeosols must have developed relatively rapidly. The interbedded thin trachyte flows are interpreted as agglutinate flows. The isolated lenses probably represent either a distal air-fall equivalent of an agglutinate flow or an air-fall of lower volume that did not generate agglutinate flows. The well-laminated ashes with U-shaped erosion channels, rip-up blocks and pumice lapilli lenses are interpreted as dry surge deposits (Fisher 1977). If the channels were eroded by pyroclastic surges as suggested by Fisher (1977), then their orientation implies a change in eruption direction, compared to the dune-like bedforms.

Enkorika Formation (S5). This formation comprises trachyte lavas which Johnson (1969) grouped with the Oloolwa Formation agglutinate flows. However, at two localities on the north flank, they clearly overlie Esinoni Formation pumice-lapilli tuffs. The Enkorika Formation is assumed to be syn-caldera I in age because it is trachytic in composition. However, the exact relationship to caldera I collapse is uncertain. The low-volume trachyte lava flows and domes were erupted from the N-S orientated Enkorika fissure zone on the north flank (Fig. 2). This zone extends from the landslipped area at Kisharu to the trachyte scoria cone, Tandamara (Fig. 2). The oldest lava flows extend up to 1.5 km on either side of the fissure. Later, at least 14 lava domes were emplaced along the zone. The flows and domes are both fine-grained, poorly-vesiculated trachytes. The stubby flow morphology and the association with lava domes indicates a relatively high emplacement viscosity.

Post-caldera I volcanism (*S6–S8*). Post-caldera I deposits are divided into three formations (S6-S8). The S8 formation and the youngest part of the S7 formation post-date caldera II collapse.

Entarakua Formation (*S6*). This formation comprises phonolite lava flows and an air-fall ash erupted from vents on the floor of caldera I, and ponded against its north and west margins (Fig. 8). To the south and east, the lavas overstepped the caldera margins, and flowed south down the Ewaso Kedong Valley for at least 10 km (Fig. 2). The lavas are <15 m thick, with pahoehoe-surfaces and numerous pressure ridges. A >10 km network of lava tubes, on the NE flank, has been described by Williams (1963). The phonolites contain <5% of anorthoclase phenocrysts, contrasting with up to 30% of anorthoclase megacrysts in the S7 and S8 lavas. The relatively fresh appearance of the NW Satellite Vent Flow (Johnson 1966, 1969; the Manyatta Flow of McCall & Bristow 1965) suggests it may be the youngest and pressure ridges indicate that its vent was probably situated close to Sampu Olkuo scoria cone (Fig. 2; the Manyatta cone of McCall & Bristow 1965).

A 1–25 m thick sequence of indistinctly parallel-laminated, hydrothermally-altered, air-fall ashes, represent the only post-caldera I pyroclastic activity, apart from a scoria cone on the surface of the Island Block. The ashes overlie S6 lavas and crop out only in the outer wall of the Ring Trench. They are thickest in the western wall, where they include air-fall bomb and block layers, and eastwards thin to <1 m, over a distance of 6 km. The fine grain size and hydrothermal alteration of the ashes, their localized nature, and association with bomb horizons, suggest that they may have originated by phreatomagmatic eruptions on or close to the caldera II ring-fracture.

Ol Doinyo Onyoke Formation (*S7*). The Ol Doinyo Onyoke Formation is characterized by anorthoclase-phyric phonolite lava flows. However, the anorthoclase contents, up to 30%, contrast with the relatively phenocryst-poor S6 phonolites. Two or three flows, exposed above the S6 ashes in the Ring-Trench, with only up to 10% of anorthoclase megacrysts are grouped with S7 lavas. This formation has the largest volume (Table 1), and includes all the deposits of Ol Doinyo Onyoke (Ol Doinyo Nyukie) cone (Fig. 2). It includes the lithic breccia that forms most of the Island Block and lava flows and a scoria cone on its surface.

The Ol Doinyo Onyoke cone is the highest point of Suswa and consists entirely of S7 lavas. McCall & Bristow (1965) noted that the earliest flows are more voluminous, and that they can be traced for up to 6 km to the south, and up to 4 km to the north of the cone. This probably reflects the regional southerly tilt of the rift floor, also shown by the southerly dips of S6 lavas on the east flank (Fig. 8). The S7 lavas do not extend as far as S6 lavas, which is possibly due to their higher viscosity, caused by the abundance of anorthoclase megacrysts. S7 lavas overlie the extrapolated continuation of the caldera scarp in the south and east. A pit crater, about 460m deep, with no associated deposits, developed on the cone, and was later truncated by the collapse of caldera II.

The breccia of the Island Block comprises very poorly sorted, angular blocks, up to 3m across, of anorthoclase-megaphyric lava in a hydrothermally-altered clay-rich

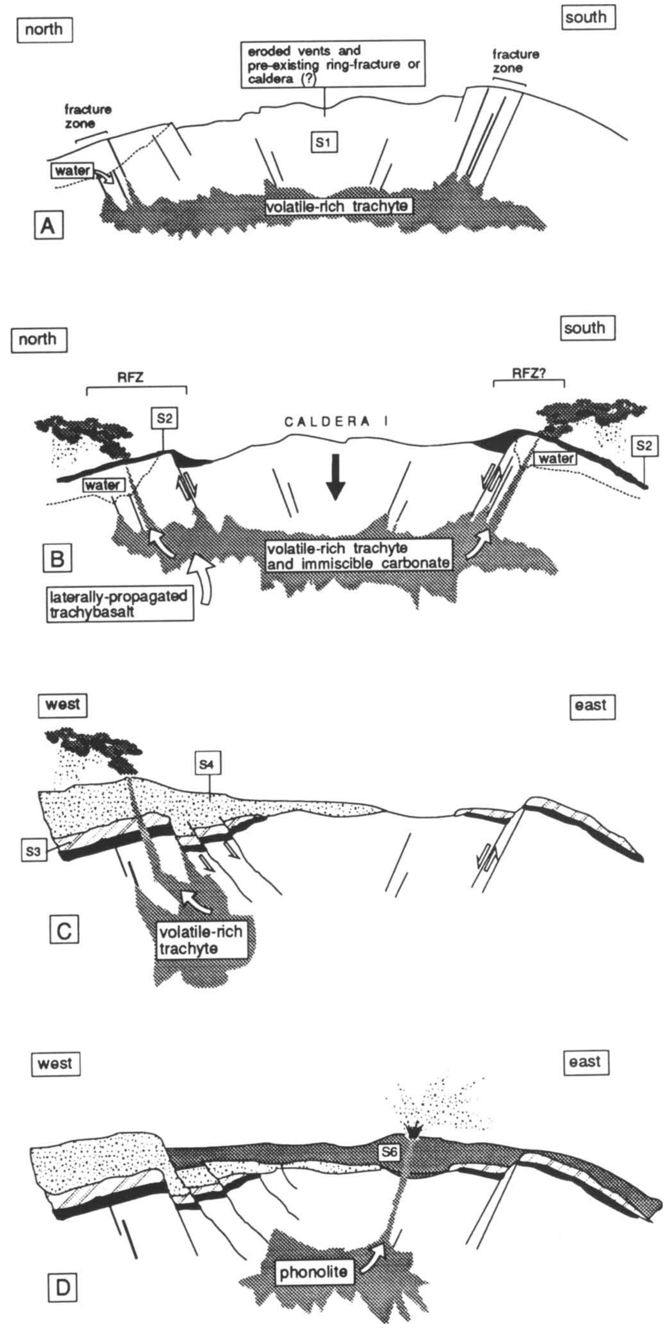

Fig. 8. Pre- to early post-caldera I history. (**A**) Development of Ring-Feeder Zone (RFZ) including caldera I ring-fault by contraction of S1 magma or ascent of S2 magma. Existence of a caldera at this stage is uncertain. (**B**) Magma-water interaction and influx of trachybasaltic magma. (**C**) Eruptions in west of caldera and subsidence of caldera floor in northwest, as a response to these eruptions; S5 lavas erupted from the Enkorika Fissure Zone (not visible). (**D**) Post-caldera phonolites (S6) erupted from vents near centre of the caldera; ponding in the west and overstepping the eastern wall.

matrix. It is interpreted as a debris flow deposit caused by large-scale collapse of Ol Doinyo Onyoke cone during development of caldera II (Fig. 9). Subsequently, lavas and a scoria cone, now exposed on the Island Block, were erupted from vents on the floor of caldera II (Fig. 9).

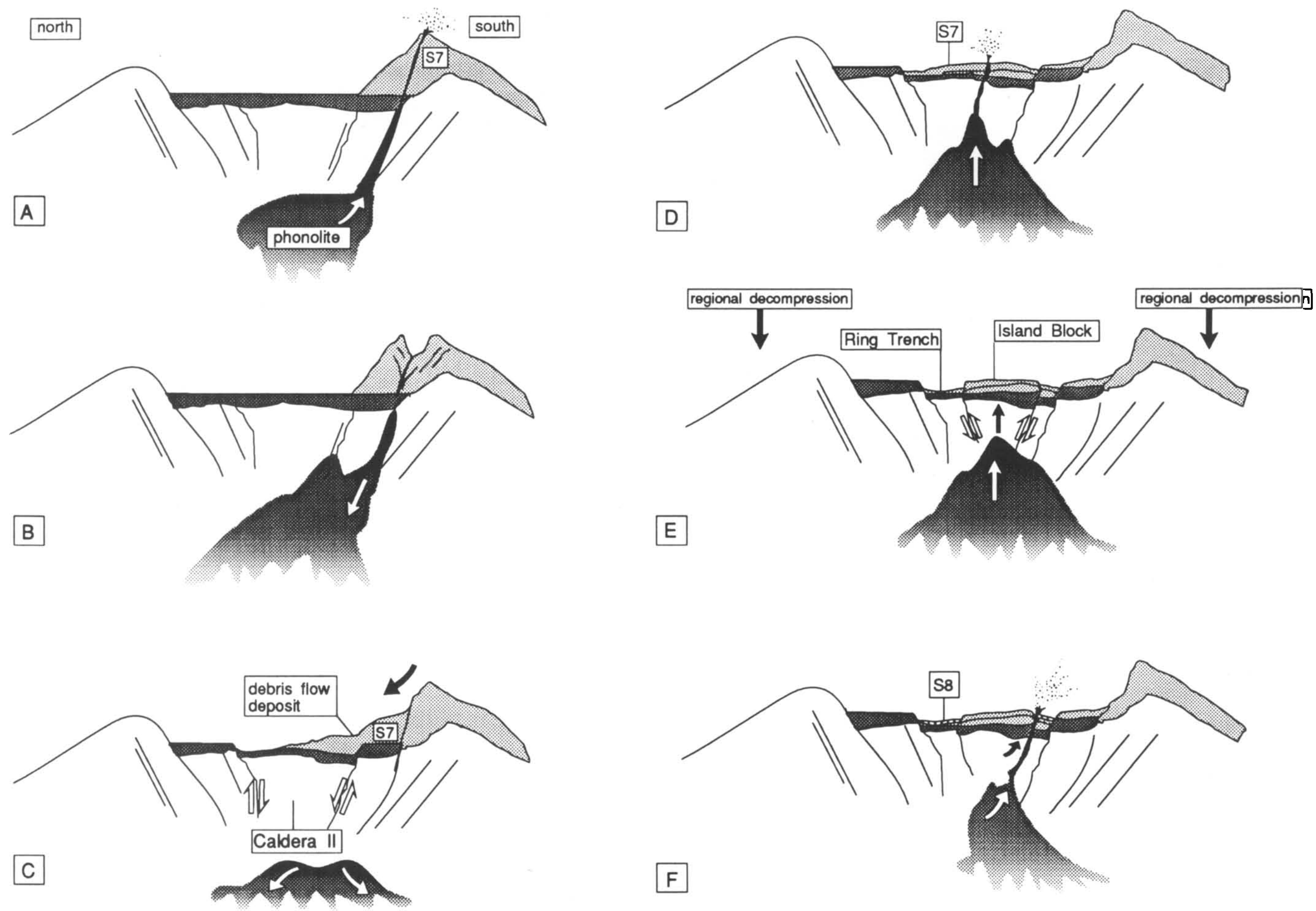

Fig. 9. Post-caldera I to recent history. (**A**) Construction of Ol Doinyo Onyoke phonolite lava cone (S7). (**B**) Formation of a pit-crater by withdrawal of magma at depth. (**C**) Continued withdrawal, truncation of cone, and formation of caldera II. (**D**) Eruption of phonolite lavas from floor of caldera II (S7). (**E**) Ring-Trench and Island Block structures developed by block resurgence of caldera floor. (**F**) Post-resurgence phonolite lava flow eruptions (S8) from SE Ring-Trench floor and south flank; tilting of Island-Block at this stage (?).

Eululu Formation (*S8*). This formation of phonolite lava flows, on the floor of the Ring Trench and a single flow on the south flank (Fig. 2), is the youngest magmatic activity on Suswa. The flows are lithologically identical to S7 lavas.

Volume estimates.

Volume estimates for each formation are given in Table 1. The dense rock equivalent (DRE) is assumed to represent half the actual volume for pyroclastic deposits. Half of the volume of S2 ignimbrites is assumed to have been transported as fine ash (Sparks & Walker 1977) and deposited outside of the area. Air-fall pyroclastics are assumed to be block wedges, with their maximum thickness as the highest part of the wedge, and a radial distribution about the inferred vent. A sixth of unconsolidated or poorly consolidated pyroclastics is assumed to have been removed by fluvial/aeolian erosion. This figure is based on an estimate of six times the volume of in situ pyroclastics on Suswa to reworked pyroclastics on the lower flanks and surrounding plains. Details of volume estimates for individual deposits are given in Skilling (1988).

Caldera development at Suswa

Suswa has two calderas. Caldera I is the largest and has a complex history of collapse. Caldera II collapsed within caldera I and is characterized by a Ring Trench and Island Block structure (Fig. 2).

Caldera I

Caldera I has a diameter of about 12 km and an extrapolated area of approximately 113 km^2. Half of the caldera wall is preserved (Fig. 2), ranging in height from 0 to 200 m, and with slopes of <20–55°. The present volume of the depression is about 13.5 km^3. An approximately 0.4 km^3 embayment, with no associated collapse debris on the caldera floor, is present in the west of caldera I (Fig. 2). The total volume of ponded postcaldera material is at least 8.5 km^3, if an average thickness of 75 m is assumed. This value is based on Ring Trench sections, where up to 75 m of S6 (post-caldera) phonolites are exposed. A caldera volume (i.e. caldera fill and depression) of 22 km^3 is estimated. This is a minimum volume, because the altitude of the precaldera volcano is uncertain and the total thickness of post-caldera fill is unknown.

The evolution of caldera I and associated syn-caldera eruptive activity was particularly complex in the initial stages. Unlike Menengai (Leat 1984) and Longonot (Scott 1980), no large-volume ash-flow sheets have been distinguished. At Suswa, repeated low-volume deposits suggests that caldera collapse was incremental. Initially, S2 magmas were erupted, probably from the zone of arcuate fractures, termed the Ring-Feeder Zone (RFZ, Fig. 2). The Ring-Feeder Zone was the source both of the S3 and S4 agglutinate flows. It is unclear whether the zone developed because of a response to drainage of the S1 magma, or by updoming caused by ascending S2 magma (cone-sheet fractures). However, it is pertinent that syn-caldera vents lay outside the currently exposed caldera ring-fault, which suggests that the caldera collapsed on an inner ring-fracture, whilst eruptions proceeded on outer ring-fractures. Such a collapse mechanism is more easily understood if collapse occurred on a pre-existing ring-fault (Fig. 8). It also suggests, as McCall & Bristow (1965) and Johnson (1969) noted, that collapse may have triggered volcanism and not necessarily vice versa

The wide compositional variations, phreatomagmatic and pyroclastic nature of the S2 deposits emphasize the complexity of processes during or immediately preceding the initial phase of subsidence. Whilst magmatic overpressure due to volatile exsolution is important in the generation of pyroclastic eruptions, its importance as the initial trigger for destabilization of the chamber is less certain, and other factors were probably equally important. Magma–water interaction is capable of destabilizing the magma chamber. The development of the Ring Feeder Zone or the extension of fractures in a pre-existing ring-fracture system by ascending S2 magma could have allowed the influx of water (Fig. 8).

The introduction of denser trachybasaltic magma into the chamber beneath Suswa offers a second method for destabilization (Blake 1981). It is possible that the trachybasalt was derived from a zoned magma chamber beneath Suswa, but there is some evidence for lateral propagation. Magma with similar composition to the Suswa trachybasalts was erupted to the north, near Tandamara (Skilling 1988). Mixed trachyte–basalt lavas were erupted at Longonot (Fig. 2) following each of three caldera collapses (Scott & Bailey 1986) and at other localities further north along this general fissure line (Scott 1980). Though there is no evidence of magma mixing in the Suswa trachybasalts it is possible that they were completely homogenized. No trachybasalts are exposed to the immediate south of Suswa, suggesting that lateral propagation was directed southwards, perhaps along the Enkorika Fissure Zone.

Following these early low-volume eruptions, caldera collapse continued with eruptions from Ring Feeder Zone vents of S3 agglutinate flows (Fig. 2). The western distribution of the S4 pumice tuffs was attributed by McCall & Bristow (1965) and Johnson (1969) to easterly winds. However, the coarse welded air-fall tuffs suggest a vent(s) in the west of caldera I. The floor of the caldera may have been lower in the northwest, as there, the walls are presently much higher than elsewhere, and also S6 lavas overstep the caldera margin in the southeast (Fig. 8). It is possible that these relationships were inherited from the pre-collapse topography, but the vents association suggests that the caldera floor may have subsided by 'hinged subsidence' (Nappi *et al.* 1991) or by 'trapdoor uplift' (Mahood & Hildreth 1983) of the southern part as a response to eruptions in this area.

The rarity of embayments in the present caldera I ring-fault suggests that the caldera collapsed as a coherent piston-like block (Valles-type collapse). The scalloped embayment in the west (Fig. 2) truncates the entire S4 sequence, which was erupted from vents in this area. Post-caldera I lavas mask any collapse breccias and the embayment may reflect either collapse of vents prior to the eruption of S6 lavas, or just a function of an irregularity in the caldera walls in the latter stages of subsidence.

The large discrepancy between the estimated original caldera I volume of at least 22 km^3 and the estimated 6 km^3 (Dense Rock Equivalent) of syn-caldera deposits (Table 1) is problematic. It is possible that more S2 deposits are present, to the east of the area mapped (Fig. 2), but none have been recorded. Winnowing of the fine ash fraction during eruption or the erosion and removal of unconsolidated pyroclastic deposits after emplacement is unlikely to account for such a large discrepancy. It is proposed that magma drainage at depth is the most plausible explanation.

Post-caldera I volcanism

The earliest post-caldera I lavas (S6) were erupted from the floor of caldera I but their vents were obliterated either during caldera II collapse, or by the construction of Ol Doinyo Onyoke cone. The youngest S6 material, represented by the NW Satellite Vent Flow, was erupted from the northwestern part of the caldera floor, which indicates that the Ring Feeder Zone, was no longer an influence on magma access to the surface. This observation concurs with that made by Walker (1984), namely that post-caldera magmas are more likely to utilize caldera floor vents than ring-fractures.

S7 lavas were erupted from a central vent on the floor of caldera I, which subsequently was the source of the Ol Doinyo Onyoke lava cone. No collapse breccias occur in the pit crater on the southern rim of this cone, suggesting that it is unlikely to have originated by explosive coring and inward collapse of the walls. The pit crater is thought to represent a precursor phase of subsidence prior to the larger collapse of caldera II (Fig. 9).

Caldera II

Caldera II has a diameter of about 5.5 km, covers an area of approximately 21 km^2, and is concentric with caldera I. It consists of an annular trench (Ring Trench) surrounding a central, tilted block (Island Block). If an average wall height of 150 m is assumed, then the present volume of the depression, neglecting the Island Block, is about 13 km^3. The Ring Trench varies in width from <0.5 km to 1.5 km. The inclination of the ring-fault is uncertain, but the walls of the Ring-Trench dip into the caldera at 40–60°. The Island Block is broadly elliptical in plan, with an area of about 9 km^2. Assuming elliptical block form and an average height of 100 m, the volume is estimated to be 3 km^3. It is tilted at <10° to the northwest, and has landslipped/step-faulted margins, particularly in its eastern and southern parts. The caldera subsided entirely due to withdrawal of magma, as no syn-caldera deposits have been recognized. Collapse truncated the lava cone and its pit crater, and generated a collapse breccia on the floor of the caldera (Fig. 9).

Johnson (1966, 1969) considered three possible origins for the Ring Trench and Island Block, two of which involved Ring Trench subsidence and, the other, caldera collapse followed by resurgence of a central block. This last mechanism is considered to be the most plausible. Successions on opposite sides of the Ring Trench cannot be correlated. This does not exclude a trench subsidence model, as caldera collapse could have occurred prior to trench subsidence. However, extensive hydrothermal alteration on the inner fault, its absence on the outer fault, and landslips only on the Island Block side, suggests that faults are of different age, and the Island Block formed by resurgence.

However, caldera II is unusually small for a resurgent cauldron. If the volume of the magma chamber was approximately that of the caldera, it would most likely have solidified prior to resurgence (Marsh 1984). It is possible that decompression caused by regional extension contributed to resurgence (Fig. 9). The tilting of the Island Block could indicate either hinged subsidence or hinged uplift of the cauldron block(s) prior to resurgence, hinged uplift of the Island Block, or could have been inherited from a tilted caldera I floor. The concentration of fumaroles within step-like landslips on the northern margin of the Island Block (Clarke *et al.* 1990) suggests the 'simple shearing block resurgence' model of Orsi *et al.* (1991), and the block was tilted on uplift. However, implicit in this model is that post-resurgence magmas would erupt on the least-uplifted side, which is not the case at Suswa.

Discussion

Caldera I collapsed as a result of a series of low-volume eruptions, accompanied by gradual withdrawal of magma at depth. Incremental collapse of various origins has been proposed for several calderas (Williams 1941; Macdonald 1972; Walker 1984; Nappi *et al.* 1991). Collapse as a consequence of magma withdrawal is also a well established idea for Hawaiian calderas (Williams 1941; Macdonald 1972), and has been inferred for centres in Iceland (Sigurdsson & Sparks 1978). The Enkorika Fissure Zone, Tandamara, the centres of calderas I and II, and the pit crater on Ol Doinyo Onyoke cone are aligned with the regional N–S normal faults. Soitamrut cone and associated lava domes on the southeast flank of Suswa are also N–S orientated. N-S orientated fissures exerted control on the siting, draining and recharge of magma chambers, overiding ring-faults or fractures. In such a tectonic setting as Suswa, these faults would be activated during episodes of extension. Large volumes of magma could be withdrawn and stored along such fissure systems, which are ubiquitous to the south of Suswa (Baker *et al.* 1988). Extension could also provide a trigger for caldera resurgence if the local magma supply was not able to drain, as was probably the case with caldera II. Further support for regional tectonics as the fundamental control on caldera collapse is the occurrence of Longonot late syn-caldera pumice interbedded with S2 pyroclastics on Suswa. This suggests that caldera collapse at both centres may have been contemporaneous and was not just a local event. Lateral propagation of trachybasaltic magma during the early stages of caldera I collapse at Suswa, may also have been caused by extension.

Conclusions

Suswa is an unusual trachyte–phonolite caldera volcano with a unique combination of structural and volcanological features, which offer an insight into caldera development and resurgence mechanisms in an extensional setting. Destabilization of the magma chamber and the subsequent collapse of caldera I was due to a combination of magmatic overpressure from volatile exsolution, explosive expansion due to interaction with water, influx of denser magma, and drainage of magma at depth. Regional extension probably provided a trigger for the latter two processes, but a chronological sequence of all these events, their inter-relationships and relative contributions to the initiation and continuation of subsidence is uncertain. Caldera II collapsed entirely due to magma withdrawal, and was later associated with block resurgence, perhaps due largely to decompression during regional extension.

I am grateful to R. Macdonald and L.A.J. Williams for help given during this work, which was undertaken during tenure of a NERC studentship. Criticisms of earlier versions of this manuscript by R. Macdonald and J.L. Smellie are gratefully acknowledged. Correspondence may be sent to the author by Fax: 0223 62616.

References

Baker, B.H., Mitchell, J.G. & Williams, L.A.J. 1988. Stratigraphy, geochronology and volcano-tectonic evolution of the Kedong-Naivasha-Kinangop region, Gregory Rift Valley, Kenya. *Journal of the Geological Society, London*, **145**, 107–116.

Bateson, J.H. 1965. Accretionary lapilli in a geosynclinal environment. *Geological Magazine*, **102**, 1–7.

Blake, S. 1981. Volcanism and the dynamics of open magma chambers. *Nature*, **289**, 783–785.

Clarke, M.C.G., Woodhall, D.G., Allen, D. & Darling, G. 1990. *Geological, volcanological and hydrogeological controls on the occurrence of geothermal activity surrounding Lake Naivasha, Kenya*. British Geological Survey-Kenya Ministry of Energy report, Nairobi.

Fisher, R.V. 1977. Erosion by volcanic base-surge density currents: U-shaped channels. *Geological Society of America Bulletin*, **88**, 1287–1297.

Gibson, I.L. 1970. Pantelleritic welded ash flow tuff from the Ethiopian Rift Valley. *Contributions to Mineralogy and Petrology*, **73**, 105–117.

—— 1974. Blister caves associated with an Ethiopian volcanic ash-flow tuff. *Studies in Speleology*, **2**, 225–232.

Hamilton, D.L., Freestone, I.C., Dawson, J.B. & Donaldson,.H. 1979. Origin of carbonatites by liquid immiscibility. *Nature*, **279**, 52–54.

Hay, R.L. & Hildreth, W. 1976. Globule ignimbrites in Kenya. *Geological Society of America Abstracts with Programs*, **8**, 589.

——, —— & Lambe, R.N. 1979. Globule ignimbrite of Mount Suswa, Kenya. *Geological Society of America Special Paper*, **80**, 167–175.

Heiken, G. & Lofgren, G. 1971. Terrestrial glass spheres. *Geological Society of America Bulletin*, **82**, 1045–1050.

Johnson, R.W. 1966. *The volcanic geology of Mount Suswa, Kenya*. PhD thesis, University of London.

—— 1968. The volcanic globule-rock from Mount Suswa, Kenya. *Geological Society of America Bulletin*, **79**, 647–652.

—— 1969. Volcanic geology of Mount Suswa, Kenya. *Philosophical Transactions of the Royal Society of London*, **265**, 383–412.

Keller, J. 1981. Carbonatitic volcanism in the Kaiserstuhl alkaline complex: evidence for highly fluid carbonatitic magmas at the Earth's surface. *Journal of Volcanology and Geothermal Research*, **9**, 423–431.

Leat, P.T. 1984. Geological evolution of the trachytic caldera volcano Menengai, Kenya Rift Valley. *Journal of Geological Society of London*, **141**, 1057–1069.

Le Masurier, W.E. 1990. Mount Sidley. *In*: LeMasurier, W.E. & Thomson, J.W. (eds) *Volcanoes of the Antarctic Plate and Southern Oceans*. American Geophysical Union Antarctic Research Series, **48**, 203–207.

—— & Kawachi, Y. 1990. Mount Hampton. *In*: LeMasurier, W.E. & Thomson, J.W. (eds) *Volcanoes of the Antarctic Plate and Southern Oceans*. American Geophysical Union Antarctic Research Series, **48**, 203–207.

LORENZ, V. 1974. Vesiculated tuffs and associated features. *Sedimentology*, **21**, 273–291.

LOWE, D.R. & KNAUTH, L.P. 1978. The oldest marine carbonate ooids reinterpreted as volcanic accretionary lapilli, Onverwacht Group, South Africa. *Journal of Sedimentary Petrology*, **48**, 709–722.

MACDONALD, G.A. 1972. *Volcanoes*. Englewood Cliffs, New Jersey, Prentice-Hall.

MACDONALD, R. 1987. Quaternary perlalkaline silicic rocks and caldera volcanoes of Kenya. *In*: FITTON, J.G. & UPTON, B.G.J. (eds) Alkaline Igneous Rocks. Geological Society, London, Special Publications, **30**, 313–333.

——, KJARSGAARD, B.A., SKILLING, I.P., DAVIES, G.R. & HAMILTON, D.L. 1993. Liquid immiscibility between trachyte and carbonate in ash flow tuffs from Kenya. *Contributions to Mineralogy and Petrology* (in press).

MAHOOD, G.A. & HILDRETH W. 1983. Nested calderas and trapdoor uplift at Pantelleria, Strait of Sicily. *Geology*, **11**, 722–726.

MARSH, B.D. 1984. On the mechanics of caldera resurgence. *Journal of Geophysical Research*, **89**(B10), 8245–8251

MCCALL, G.J.H.. & BRISTOW, C.M. 1965. An introductory account of Suswa volcano, Kenya. *Bulletin Volcanologique*, **28**, 333–367.

MOORE, J.G. & KYLE, P.R. 1990. Mount Erebus. *In*: LEMASURIER, W.E. & THOMSON, J.W. (eds) *Volcanoes of the Antarctic Plate and Southern Oceans*. American Geophysical Union Antarctic Research Series, **48**, 203–207.

NAPPI, G., RENZULLI, A. & SANTI, P 1991. Evidence of incremental caldera growth in the Vulsinian calderas (central Italy). *Journal of Volcanology and Geothermal Research*, **47**, 13–31.

ORSI, G, GALLO, G & ZANCHI, A. 1991. Simple-shearing block resurgence in caldera depressions: a model from Pantelleria and Ischia. *Journal of Volcanology and Geothermal Research*, **47**, 1–11.

SCHMINCKE, H.U. 1972. Froth flows and globule flows in Kenya. *Die Naturwissenschaften*, **11**, 1–2.

—— 1974. Volcanological aspects of peralkaline silicic welded ash-flow tuffs. *Bulletin Volcanologique*, **38**, 594–636.

SCOTT, S.C. 1980. The geology of Longonot volcano, central Kenya. *Philosophical Transactions of the Royal Society of London*, **296**, 437–465.

—— & BAILEY, D.K. 1986. Coeruption of contrasting magmas and temporal variations in magma chemistry at Longonot volcano, central Kenya. *Bulletin Volcanologique*, **49**, 849–873.

SHERIDAN, M.F. 1976. Fumarolic mounds and ridges of the Bishop Tuff, California. *Geological Society of America Bulletin*, **81**, 851–868.

SIGURDSSON, H. & SPARKS, S.R.J. 1978. Lateral magma flow within rifted Icelandic crust. *Nature*, **274**, 126–130.

SKILLING, I.P. 1988. *The geological evolution of Suswa volcano, Kenya*. PhD thesis, University of Lancaster.

SPARKS, S.R.J. & WALKER, G.P.L. 1977. The significance of vitric-enriched air-fall ashes associated with crystal-enriched ignimbrites. *Journal of Volcanology and Geothermal Research*, **2**, 329–341.

WALKER, G.P.L. 1983. Ignimbrite types and ignimbrite problems. *Journal of Volcanology and Geothermal Research*, **17**, 65–88.

WALKER, G.P.L. 1984. Downsag calderas, ring faults, caldera sizes and incremental caldera growth. *Journal of Geophysical Research*, **89**(B10), 8407–8416.

WILLIAMS, H. 1941. Calderas and their origin. *University of California Department of Geological Sciences Bulletin*, **25**, 239–346.

WILLIAMS, L.A.J. 1963. Lava tunnels on Suswa Mountain, Kenya. *Nature*, **199**, 348–350.

——, MACDONALD, R & CHAPMAN, G.R. 1984. Late Quaternary caldera volcanoes of the Kenya Rift Valley. *Journal of Geophysical Research*, **89** (B10), 8553-8570.

WILSON, C.J.N. 1980. The role of fluidisation in the emplacement of pyroclastic flows: an experimental approach. *Journal of Volcanology and Geothermal Research*, **8**, 231–249.

—— & WALKER, G.P.L. 1982. Ignimbrite depositional facies: the anatomy of a pyroclastic flow. *Journal of the Geological Society of London*, **139**, 581–592.

WOHLETZ, K.H. 1983. Mechanisms of hydrovolcanic pyroclast formation: grain-size, scanning electron microscopy and experimental studies. *Journal of Volcanology and Geothermal Research*, **17**, 31–63.

ZIMANOWSKI, B., VOLKER, L. & FROHLICH, G. 1986. Experiments on phreatomagmatic explosions with silicate and carbonatitic melts. *Journal of Volcanology and Geothermal Research*, **30**, 149–153.

Received 26 June 1992; revised typescript accepted 11 February 1993.